View Article Online / Journal Homepage / Table of Contents for this issue

Chiral and achiral linear coordination polymers from aldaric acids†

Brendan F. Abrahams,* Martin J. Grannas, Laura J. McCormick, Richard Robson* and Peter J. Thistlethwaite

Received 22nd January 2010, Accepted 6th April 2010
DOI: 10.1039/c001505a

The structures of a series of 1D coordination polymers in which divalent centres are bridged by saccharate or mucate anions are presented. In each structure the coordination environment of the metal centres is completed by a 1,10-phenanthroline or 2,2′-bipyridine ligand. Hydrogen bonding between infinite parallel chains leads to a 2D network in each structure with the aromatic groups extending above and below this plane. These groups serve as pillars between the hydrogen-bonded sheets. π–π interactions occur between aromatic groups on neighbouring parallel sheets. In most cases narrow channels filled with disordered water molecules are formed between the aromatic groups on the sides and the hydrogen-bonded sheets that lie above and below. CO_2 sorption studies on two compounds are also reported.

Published on 07 mai 2010. Downloaded on 24.02.2026 20:39:13.

Introduction

Aldaric acids are dicarboxylic acids obtained from the partial oxidation of aldohexoses. They are appealing as building blocks for the generation of coordination networks as they bind to metal centres strongly and possess a number of hydroxyl groups that may act as donors to metal centres or form hydrogen bonds that support network formation. Their use as molecular bridges between metal centres in coordination networks is also appealing because of the fact that they could be produced from a renewable resource and could be produced very cheaply if required on a large scale. Furthermore, as derivatives of sugars they are biodegradable—an attractive feature from an environmental perspective.

A number of structural investigations of metal saccharates and mucates have been undertaken.[1–25] In 2003 we showed that dianions of saccharic acid (H_2sacc, **I**), which may be obtained by the oxidation of glucose, combine with zinc ions to form a 3D network that is able to act as a host system for a wide range of molecular guests. This structure is particularly robust showing exchange of guests with retention of single crystal character. As a result of the inclusion of the chiral saccharate anion, the network is also chiral. Mucate is the dianion of the dicarboxylic acid, mucic acid (H_2muc, **II**), obtained from the oxidation of galactose. Although the parent aldohexose, galactose, is chiral, mucate is a *meso* anion. When combined with lanthanide ions it forms both 2D and 3D achiral coordination networks.[24]

Encouraged by the formation of other networks involving these anions we have extended our study to include investigations

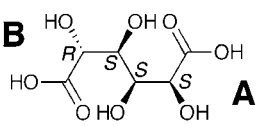

I

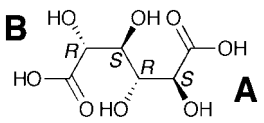

II

of metal aldarates with neutral co-ligands, in particular 2,2′-bipyridine (bipy) and 1,10-phenanthroline (phen). Such ligands are expected to block coordination sites on the metal ions resulting in a decrease in the dimensionality of the polymeric species. If 1D polymers were to form, there exists the possibility of creating materials where polymer chains are linked by hydrogen bonding into networks. Oligomeric rings could possibly also form, offering the prospect of asymmetric cavities where chiral bridging aldarate anions are involved. In addition to hydrogen-bonding interactions between the anticipated species, association of the aromatic ligands is likely to occur, either through edge-to-face or face-to-face interactions. These interactions may be expected to be significant structure-directing influences. In regard to these mixed ligand species we note the formation of a 1D coordination polymer when Cu(II) is combined with mucate and bipy to form Cu(muc)(bipy).[25]

For both of the aldaric acids considered in this report, the stereochemistry of each aldarate ligand arises from the four non-terminal C centres, each of which is asymmetric. The configuration of each asymmetric centre is indicated in **I** and **II**. In saccharic acid the two ends of the molecule are intrinsically different with one carboxylate bound to a C centre with an *S* configuration and the other bound to a C centre with *R* configuration. For the purposes of comparison within this report the two ends of the molecule are referred to as the **A** and **B** termini respectively. Similarly, in mucic acid, the end of the molecule that has the carboxylate bound to a C centre with *S* configuration is the **A** terminus, while the carboxylate bound to the C centre with *R* configuration is the **B** terminus.

Results and discussion

Aqueous solutions of potassium hydrogen saccharate, the appropriate metal acetate or nitrate, and either bipy or phen were held at 70–90 °C overnight. All mucate complexes and saccharate

School of Chemistry, University of Melbourne, Victoria, 3010, Australia. E-mail: bfa@unimelb.edu.au; r.robson@unimelb.edu.au

† Electronic supplementary information (ESI) available: Powder diffraction patterns and TGA traces. CCDC reference numbers 763056–763062. For ESI and crystallographic data in CIF or other electronic format see DOI: 10.1039/c001505a

View Article Online

Published on 07 mai 2010. Downloaded on 24.02.2026 20:39:13.

complexes involving the phen ligand crystallised directly from the hot solution, whilst the copper and zinc saccharate bipyridine complexes form slowly only after the solution has cooled to room temperature.

Structural studies

The 1,10-phenanthroline saccharate complexes are essentially isostructural. The hydrated M(sacc)(phen) compounds (M = Mn, Co and Zn) crystallise in the chiral, monoclinic space group, *C*2. A comparison of the unit cell dimensions of the manganese, cobalt and zinc analogues is presented in Table 1. The following description which focuses on hydrated Mn(sacc)(phen) also applies to the zinc and cobalt analogues. Representations of the structure are presented in Fig. 1.

There are two crystallographically distinct metal centres in the asymmetric unit, each of which lies on a two-fold axis (Fig. 1a). Each metal centre is in a slightly distorted octahedral environment, coordinated by a chelating phen ligand and four oxygen atoms belonging to a pair of saccharate dianions. Each saccharate binds through a single carboxylate oxygen and a hydroxyl group belonging to the adjacent carbon atom. Mn1 has a **Δ** configuration and is bound by the **A** termini of two saccharate anions. Mn2 has a Λ configuration and is bound by the **B** termini of two saccharate anions. The carboxylate oxygen atoms are *trans* to each other while the hydroxyl groups are *cis*. The phen ligand bound to Mn2 is disordered over two different orientations of equal occupancy, slightly displaced from each other but lying in the same plane. The disorder in the phen appears to have minimal effect on the crystal packing.

In this structure, saccharate anions bridge Mn1 and Mn2 centres resulting in a 1D zig-zag polymer as shown in Fig. 1b. Extensive hydrogen-bonding between parallel chains leads to a 2D hydrogen-bonded network (Fig. 1c) that extends in the *a*–*c* plane. Ordered and disordered water molecules also associate with these chains and assist in providing hydrogen bond bridges between the chains. The 2-fold axes that pass through the Mn centres are normal to this average plane. The phen ligands, which are all parallel, extend in directions above and below this hydrogen-bonded sheet. A representation of the sheet showing the phen ligands but with the saccharate ligands represented by single long connections is presented in Fig. 1d. This figure indicates that all phen ligands lie in parallel planes that are slightly inclined to the plane defined by Mn1 and Mn2 centres within a single chain.

The chains in neighbouring sheets have the same orientation and are symmetry related to these sheets by a pure translation (½ + *x*, ½ + *y*, *z*). The average planes of the sheets are separated by half the *b* axis *i.e.* 12.7859(2) Å. The phen ligands from parallel sheets interdigitate in a manner that leads to infinite π-stacking arrays between upward and downward pointing aromatic groups (Fig. 1e). With the phen ligands serving as pillars between the hydrogen bonded sheets, narrow channels between the aromatic ligands are formed (Fig. 1f). These channels are occupied by ordered and disordered water molecules.

Cd(muc)(phen) was prepared in a reaction between cadmium nitrate, mucic acid, potassium hydroxide and 1,10-phenanthroline in water at 77 °C. A remarkable structural similarity exists between the saccharate complexes M(sacc)(phen) (M = Co, Mn, Zn) and the compound Cd(muc)(phen) despite the fact that

Table 1 Crystal data and refinement detail

Compound	Mn(phen)(sacc)·2.25H_2O	Zn(phen)(sacc)·2H_2O	Co(phen)(sacc)·2H_2O	Cd(phen)(muc)·H_2O	Cu(phen)(muc)·3H_2O	Cu_2(bipy)$_2$(sacc)$_2$·9H_2O	Zn_2(bipy)$_2$(sacc)$_2$·7H_2O
Formula	$C_{18}H_{20.5}MnN_2O_{10.25}$	$C_{18}H_{20}N_2O_{10}Zn$	$C_{18}H_{20}CoN_2O_{10}$	$C_{18}H_{20}CdN_2O_{20}$	$C_{18}H_{22}CuN_2O_{11}$	$C_{32}H_{50}Cu_2N_4O_{25}$	$C_{32}H_{46}N_4O_{23}Zn_2$
M	483.81	489.75	483.30	536.76	505.92	1017.84	989.21
T/K	130(2)	130(2)	130(2)	130(2)	130(2)	130(2)	130(2)
Crystal system	Monoclinic	Monoclinic	Monoclinic	Monoclinic	Monoclinic	Triclinic	Orthorhombic
Space group	*C*2	*C*2	*C*2	*C*2/*c*	*P*2/*c*	*P*1	$P2_12_12_1$
a/Å	8.09180(10)	8.0660(2)	8.0565(4)	7.9270(19)	9.7117(3)	6.953(2)	10.9528(2)
b/Å	25.5718(3)	25.1855(6)	25.1374(8)	25.9288(45)	10.2821(2)	12.209(4)	13.6506(2)
c/Å	9.95990(10)	9.8493(6)	9.8567(4)	10.2343(20)	10.9564(4)	13.829(4)	26.0918(4)
α/°	90	90	90	90	90	111.295(6)	90
β/°	111.096(2)	110.551(3)	110.482(5)	112.785(1)	113.107(4)	97.980(5)	90
γ/°	90	90	90	90	90	102.352(6)	90
V/Å^3	1922.80(4)	1873.51(9)	1869.98(13)	1930.8(8)	1006.30(5)	1037.8(6)	3901.04(11)
Z	4	4	4	8	4	1	4
μ/mm^{-1}	6.198	2.410	7.832	9.594	4.340	1.123	2.382
Unique reflections	2393	2398	2160	1259	1573	5223	5502
R_{int}	0.0413	0.0261	0.0429	0.0834	0.0275	0.0171	0.0282
wR_2 (F^2, all data)	0.2201	0.1346	0.1497	0.3022	0.1376	0.1319	0.1304
R_1 [$I > 2\sigma(I)$]	0.0782	0.0428	0.0556	0.1158	0.0469	0.0509	0.0435

This journal is © The Royal Society of Chemistry 2010

View Article Online

Published on 07 mai 2010. Downloaded on 24.02.2026 20:39:13.

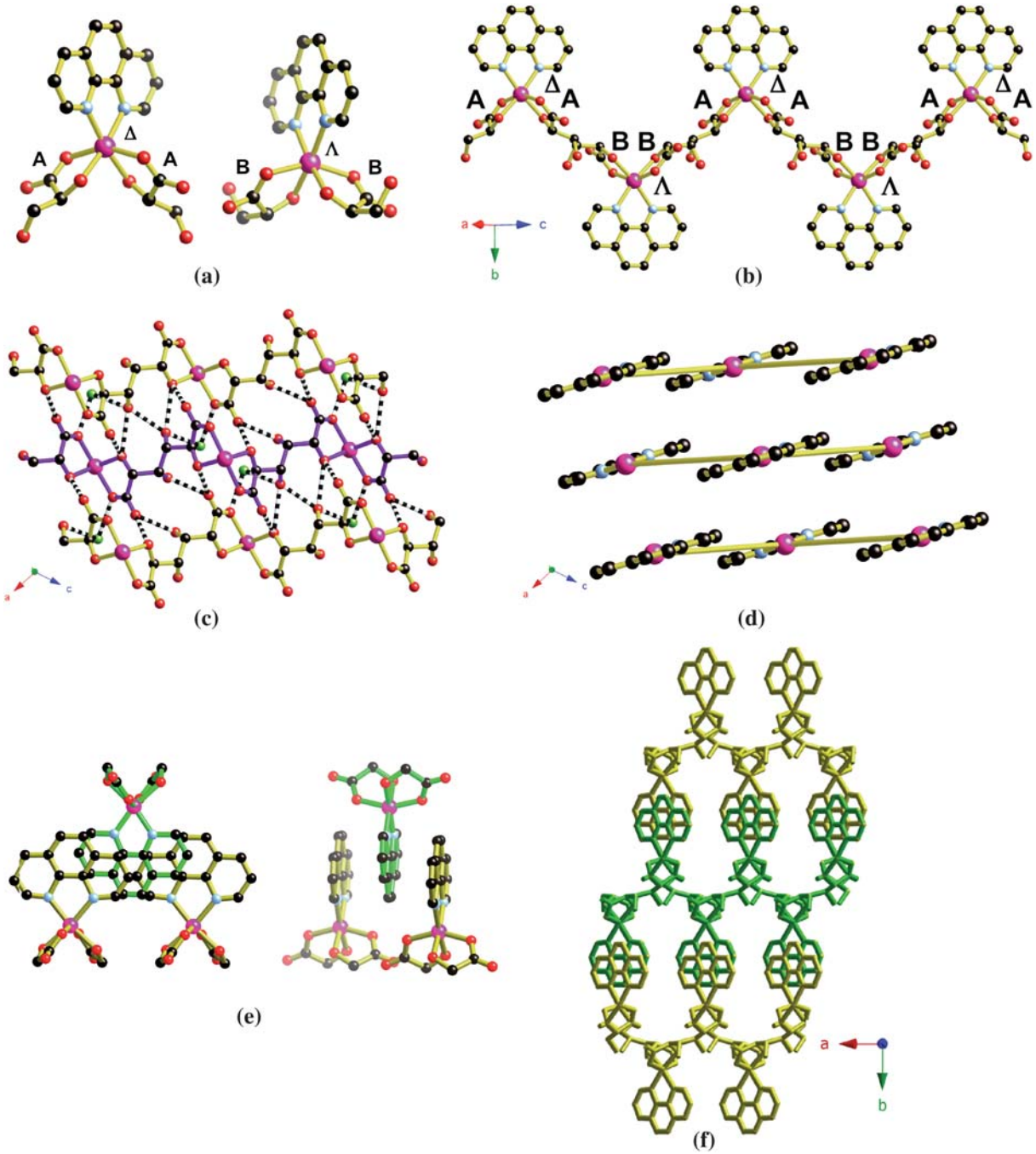

Fig. 1 The structure of Mn(sacc)(phen). (a) The coordination environments of Mn1 (left) showing the Δ configuration and Mn2 (right) showing the Λ configuration. The **A** and **B** labels refer to the two distinct ends of the saccharate dianion. The saccharate dianion has been truncated between the third and fourth C atoms. (b) Part of the 1D zig–zag Mn(sacc)(phen) polymer. The upward pointing phen ligands are bound to Mn1 centres while the downward phen ligands are bound to Mn2. (c) Part of the 2D hydrogen-bonded sheet showing three parallel chains within the one sheet; the central chain is highlighted with purple bonds. Hydrogen bonded interactions are indicated by striped connections. The green spheres represent the oxygen atom of an ordered water molecule. The phen ligands have been omitted. (d) Part of the 2D sheet with saccharate ligands represented by long gold connections. Phen ligands, which are all parallel with each other, and almost parallel with the direction of the coordination polymer, extend above and below the 2D sheet. (e) Part of an infinite stack of phen groups formed from neighbouring hydrogen bonded sheets, viewed almost normal to the aromatic planes (left) and almost parallel to the aromatic planes (right). (f) Part of the 3D structure of Mn(sacc)(phen) showing parallel channels extending along the *c*-direction. Colour code: Mn pink, O red, O (water) green, N pale blue, C black. Hydrogen atoms have been omitted for clarity.

mucate is a *meso* anion whereas saccharate is chiral. This difference appears to have very little effect on the cell dimensions, although not unexpectedly, a non-chiral space group (*C*2/*c*) is found for the Cd compound. In Cd(muc)(phen) (Fig. 2) there is only one crystallographically unique Cd centre but both Λ and Δ forms, which are related by symmetry, are present in equal numbers (Fig. 2a). As was the case with the previously described saccharate complexes the Cd centres with Δ configuration are

View Article Online

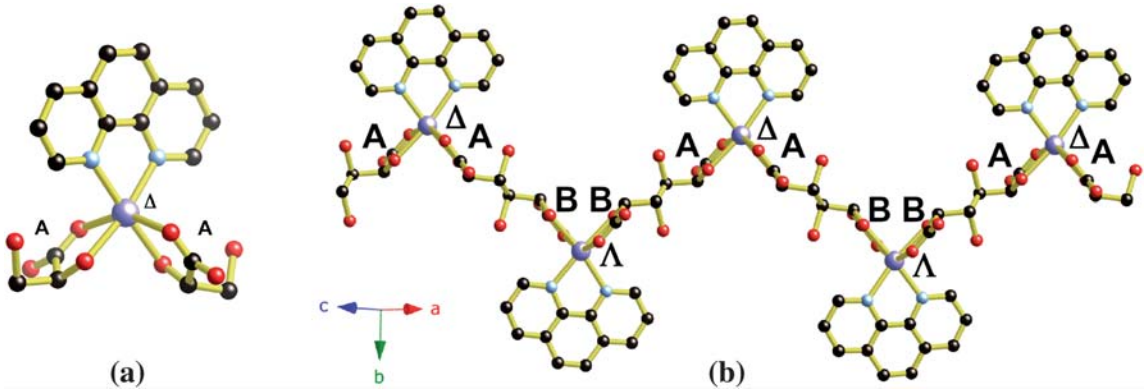

Fig. 2 The structure of Cd(muc)(phen). (a) The coordination environment of the Cd centre within Cd(muc)(phen). The Δ configuration is shown, however, the symmetry related Λ configuration is also present within the crystal. The mucate dianion has been truncated between the third and fourth C atoms. (b) Part of the 1D zig–zag Cd(muc)(phen) polymer. The **A** and **B** labels refer to the two distinct ends of the mucate dianion. Colour code: see Fig. 1 caption; Cd lavender. Hydrogen atoms have been omitted for clarity.

Published on 07 mai 2010. Downloaded on 24.02.2026 20:39:13.

bound by the **A** termini of the aldarate dianion while the Cd centres with Λ configuration are bound by the **B** termini. The zig-zag polymeric chain, represented in Fig. 2b, is similar to that found for the saccharate analogues (Fig. 1b). The phen ligand is disordered over two closely related sites, as was the case with some of the phen groups in M(sacc)(phen) (M = Co, Mn and Zn). Unlike the saccharate anion in the earlier described structures, the mucate anion exhibits a small degree of disorder associated with the positions of two non-coordinated hydroxyl groups. The structural similarity of the Cd(muc)(phen) structure with the analogous saccharate-based structures extends to the formation of the hydrogen bonded sheets and the relative orientation of the phen groups of the chains within these sheets. The interdigitation of the phen groups leading to the formation of channels is very similar to that found for M(sacc)(phen) (M = Co, Mn, Zn) (Fig. 1e and f).

Similar reactions to those described above using copper(II) acetate or nitrate with potassium hydrogen saccharate and phen yielded only a very fine brown precipitate. When heated to 80° for three days, the aqueous reaction mixture afforded blue needle crystals, which were found to be Cu(ox)(phen)·$2H_2O$ (ox = oxalate).[26] Presumably under these conditions the oxalate is generated by saccharate decomposition. Reaction of copper(II) nitrate and phen with dipotassium mucate, afforded blue block-like crystals of hydrated Cu(muc)(phen). This compound is a linear polymer in which each copper centre is coordinated by one phen ligand and a pair of bridging mucate anions (Fig. 3a). As with the earlier examples considered, chelation of the anions occurs through a carboxylate oxygen atom and an α-hydroxyl group. Along the polymeric chain, the copper centres alternate between Δ and Λ configurations, however, as with Cd(muc)-(phen) these are related by crystallographic symmetry. Unlike the structure of Cd(muc)(phen), however, the Cu centres with the Λ configuration are now bound by the **A** termini of the mucate dianions and the metal centres with the Δ configuration are bound by the **B** termini. Also in contrast to the earlier structures the carboxylate oxygen atoms are now *cis* to each other while the hydroxyl groups are *trans*. The chain has a zig-zag conformation, however, this is not as pronounced as that seen in the earlier examples. Once again, hydrogen bonding between parallel sheets results in a 2D network (Fig. 3b) with the phen ligands directed either up or down from the mean plane of the sheet. In contrast to the other phen structures, the phen ligand is in a significantly different orientation relative to the direction of the polymeric chains (Fig. 3c). Despite these differences, interdigitation of the phen groups from neighbouring sheets, leading to infinite face-to-face aromatic interactions, results in the formation of narrow, water-filled channels similar to those observed in the earlier structures (Fig. 3d). The Cu(muc)(phen) structure is very similar to that of Cu(muc)(bipy) that was determined by Saladini *et al.* in 1999.[25]

When 2,2′-bipyridine is combined with Cu(II) and saccharate, the copper complex, Cu(sacc)(bipy) is formed (Fig. 4). The structure consists of parallel 1D Cu(sacc) chains that are hydrogen bonded together to form a 2D network. Within each chain there are two types of saccharate ligand and two types of Cu(II) centres. Although crystallographically distinct, each saccharate binds in a similar manner. At one end, chelation occurs through a carboxylate oxygen and the α-hydroxyl group while at the other end a single carboxylate oxygen atom binds to a Cu(II) centre; the second oxygen of this carboxylate group forms a weak interaction with the Cu(II) centre. Taking into account this weak interaction it is possible to assign the configuration of crystallographically distinct Cu(II) centres as either Δ or Λ (Fig. 4a). The Cu centres with the Δ configuration are bound by two **B** termini while the Λ Cu centres are bound by two **A** termini. The configurations of the Cu(II) centres alternate within the 1D chains (Fig. 4b).

The bipy ligand bound to the Δ Cu(II) centre is disordered over two orientations in a manner similar to that found for the phen ligands in the earlier described compounds. A small degree of disorder is also apparent in the saccharate ligand.

Hydrogen bonds, both directly between chains and through bridging water molecules, link the chains together to form the sheets, which extend parallel to the *a*–*c* plane (Fig. 4c). Bipy units are directed upwards and downwards from the plane of the sheet, and interdigitate with the bipyridine units from the sheets situated directly above and below. The orientation of the bipy groups relative to the 1D chains is shown in Fig. 4d. Face-to-face aromatic interactions, similar to those observed in the earlier structures result

 This journal is © The Royal Society of Chemistry 2010

View Article Online

Published on 07 mai 2010. Downloaded on 24.02.2026 20:39:13.

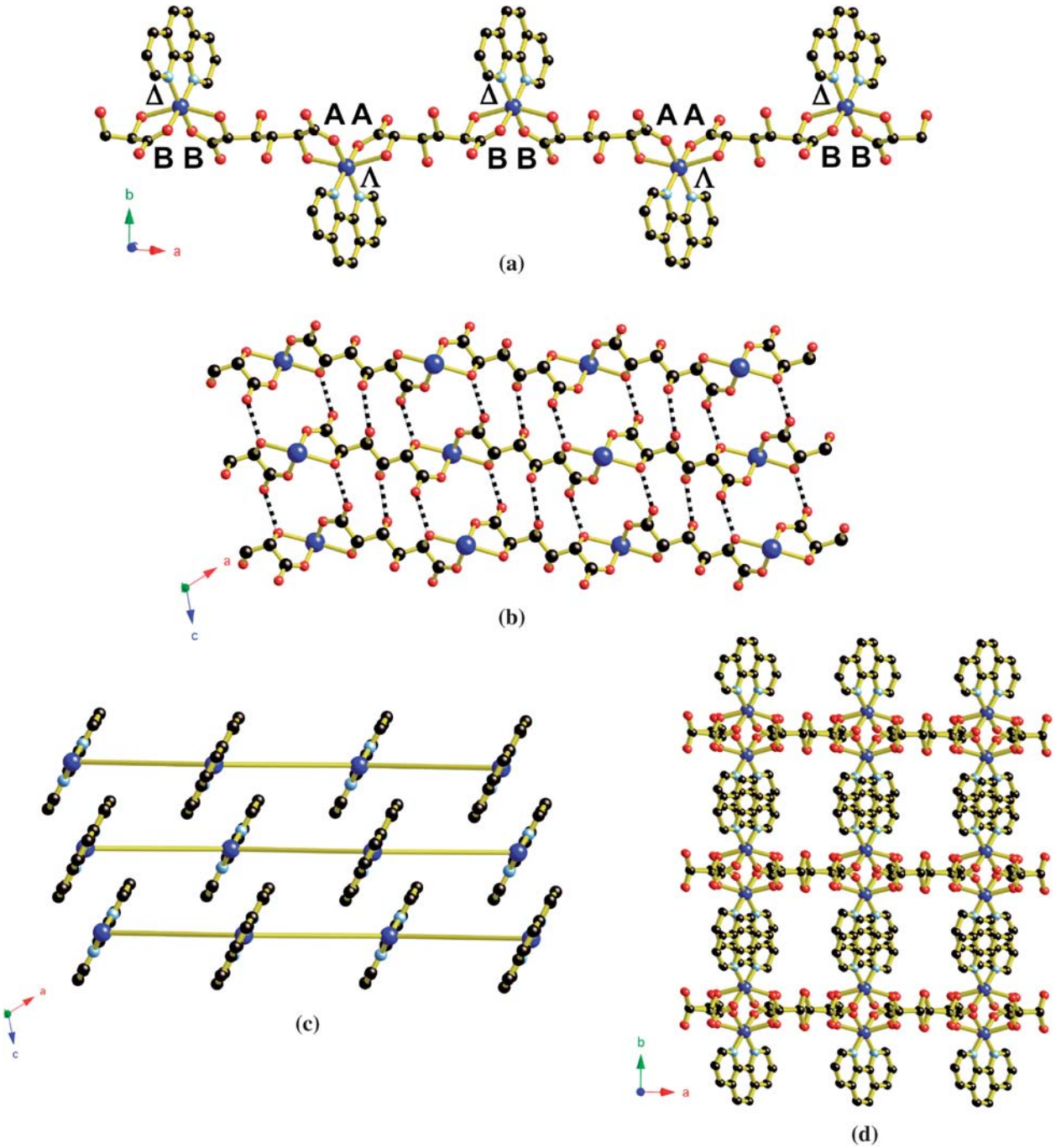

Fig. 3 The structure of Cu(muc)(phen). (a) A single Cu(muc)(phen) chain; copper centres alternate (from left) between Δ and Λ ligand arrangement. (b) Part of the hydrogen-bonded sheet formed from Cu(muc)(phen) chains. The sheet extends in *a*–*c* plane; hydrogen bonds are represented by striped connections. Phen ligands have been omitted. (c) Part of a 2D sheet showing the relative orientation of the phen ligands to the linear polymers; mucate ligands are represented by long connections. (d) A view along the channels formed between the sheets of Cu(muc)(phen). Colour code: see Fig. 1 caption; Cu blue. Hydrogen atoms have been omitted for clarity.

from the interdigitation of bipy ligands. As with the other structures narrow channels are also present between layers (Fig. 4e).

Zn(sacc)(bipy) crystallises in the chiral, orthorhombic space group $P2_12_12_1$, and like the other saccharate-based polymers described above, the asymmetric unit contains pairs of crystallographically distinct zinc centres, saccharate anions and bipy ligands. There are, however, significant differences between this structure and the other structures described in this present work.

Remarkably there are two distinct types of helices present in the structure both of which have the same composition. One is a right-handed helix (Fig. 5a), containing only Zn1 centres all of which have a Δ configuration and involving only one type of saccharate dianion, while the other is a left-handed helix (Fig. 5b) containing only Zn2 centres, all of which have a Λ configuration and involving the other type of saccharate dianion. Unlike all the previous structures considered, each of the Zn(II) centres is bound by the **A** terminus of

View Article Online

Published on 07 mai 2010. Downloaded on 24.02.2026 20:39:13.

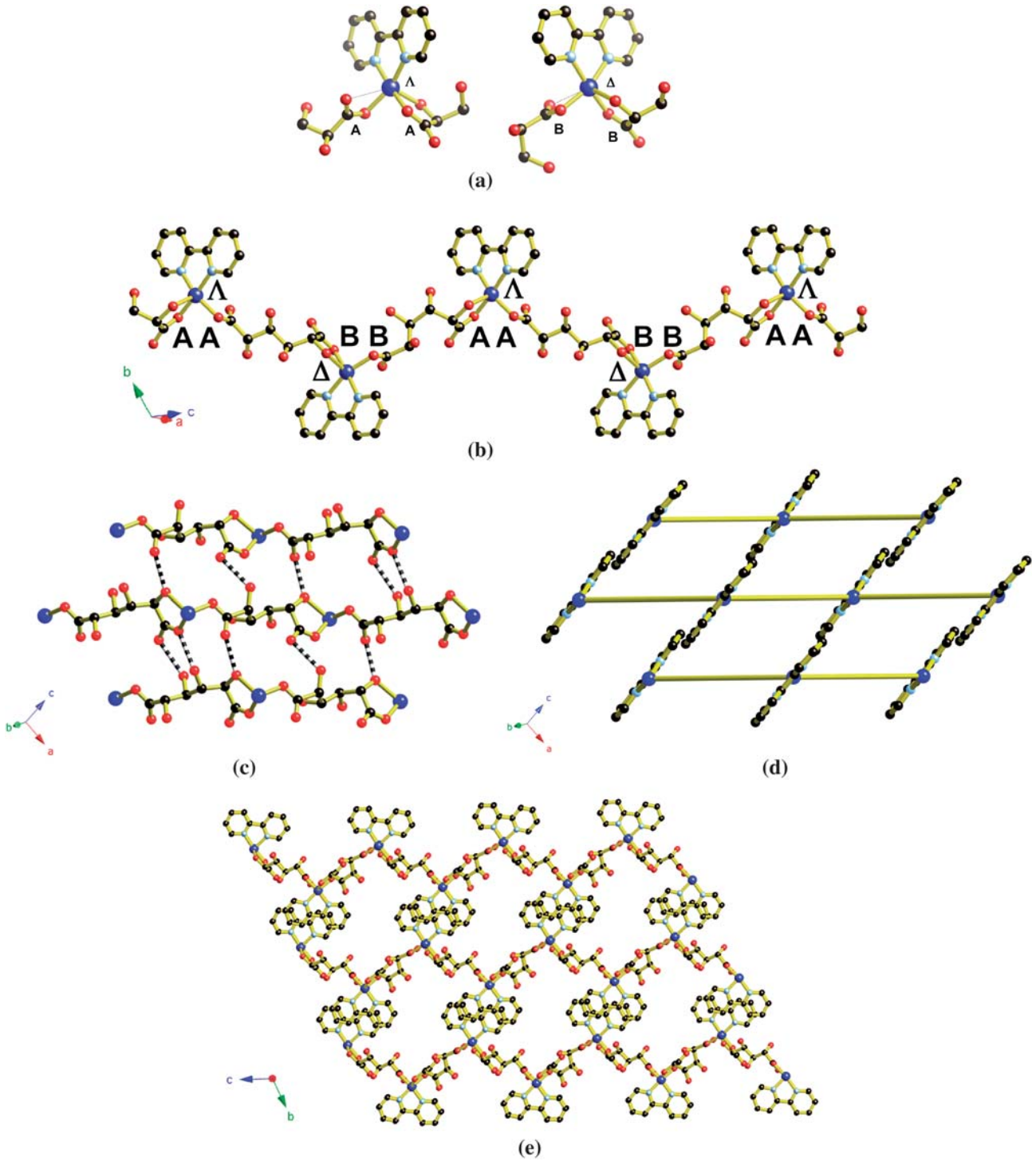

Fig. 4 The structure of Cu(sacc)(bipy). (a) The coordination environments of the two types of Cu(II) centre in the structure. (b) A section of the 1D zig–zag coordination polymer. (c) Part of the hydrogen bonded sheet formed from chains linked from hydrogen bonding (indicated by striped connections). The sheet is parallel to the *a*–*c* plane. Bipy ligands are not shown. (d) Part of the 2D sheet indicating the orientations of the bipy ligands. Bridging saccharate ligands are indicated by long connections. (e) The 3D structure viewed edge-on to the 2D sheets. Channels running parallel to the *b* direction lie between the interdigitating bipy ligands. Colour code: see Fig. 1 caption; Cu blue. Hydrogen atoms have been omitted for clarity.

one saccharate and the **B** terminus of the next saccharate within the helix. In the previously described structures each metal centre is bound by either a pair of **A** termini or **B** termini.

The helical nature of the two chains is emphasised in Fig. 5c which shows two parallel helices; the blue chain (the same chain represented in Fig. 5a) has a right hand twist while the red chain (the same chain represented in Fig. 5b) has a left hand twist. From a geometrical perspective there are significant differences between the chains, with the blue helix appearing more circular than the red helix when viewed along the helical axis.

 This journal is © The Royal Society of Chemistry 2010

View Article Online

Published on 07 mai 2010. Downloaded on 24.02.2026 20:39:13.

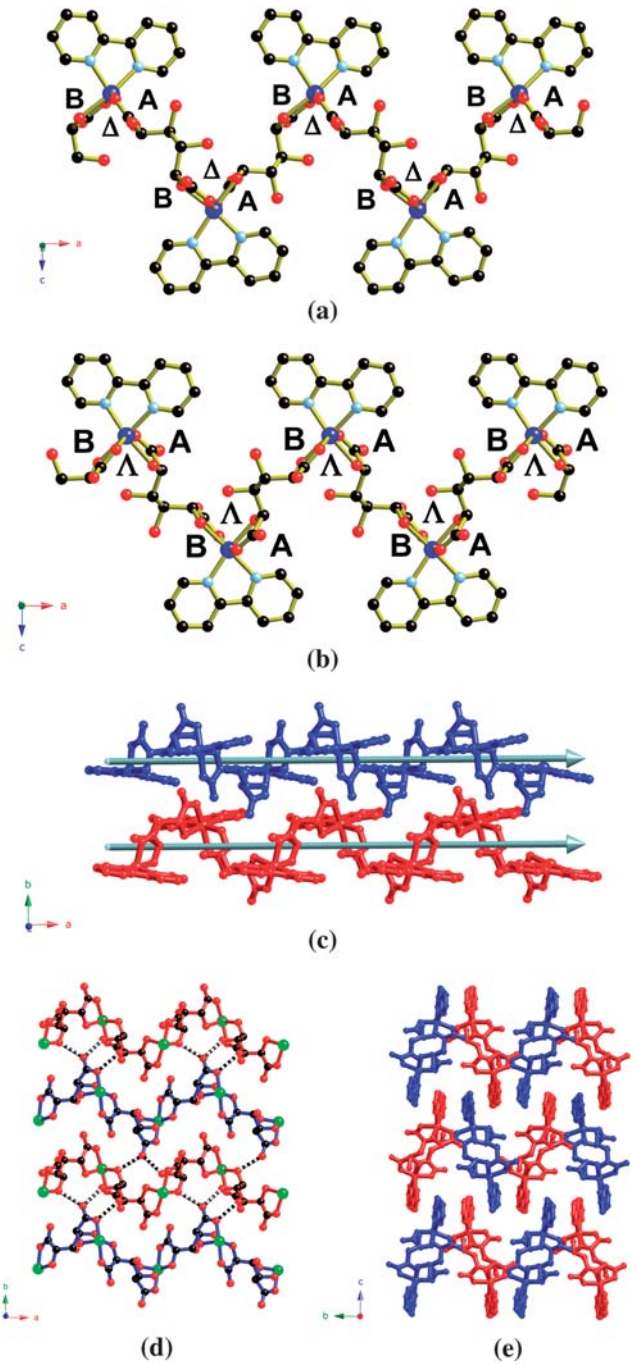

Fig. 5 The structure of Zn(sacc)(bipy). (a) A Zn(sacc)(bipy) helix containing Zn(II) centres with Δ configurations. (b) A Zn(sacc)(bipy) helix containing Zn(II) centres with Λ configurations. (c) Neighbouring helical chains of Zn(sacc)(bipy) within a hydrogen-bonded sheet. The blue chain is a right-handed helix (represented in Fig. 5a) and contains Zn(II) centres that all have the Δ configuration; the red chain is a left-handed helix (represented in Fig. 5b) and contains Zn(II) centres that all have a Λ configuration. (d) Part of the hydrogen bonded sheet extending in the *a*–*b* plane. Bipy ligands have been omitted. (e) A view along the helical axes showing the interdigitation of the bipy groups.

Hydrogen bonding between the two types of chains as represented in Fig. 5d leads to the formation of a 2D hydrogen bonded network that extends in the *a*–*c* plane. For both left-handed and right handed helices within the one sheet, the zinc saccharate sequence, which may be represented as ⋯Zn–AB–Zn–AB–Zn–AB–Zn⋯, is the same and in contrast to the other structures considered in this report where the chains are of the type ⋯M–AB–M–BA–M–AB–M⋯. The bipy ligands extend above and below the plane of this hydrogen-bonded sheet. Face-to-face π interactions involving the bipy ligands are apparent in the structure but the association of the groups is different from that observed in the earlier structures that involve the alternation of upward and downward pointing aromatic groups in infinite stacks. In the case of Zn(sacc)(bipy), a pair of almost parallel bipy groups from the same hydrogen bonded sheet associate with each other. It is this pair that now interdigitates with symmetry-related pairs from neighbouring as shown in Fig. 5e. This interdigitation does not result in the formation of the channels observed in the earlier structures. Interestingly, in neighbouring, symmetry-related, parallel sheets the chain direction is reversed *i.e.*⋯Zn–BA–Zn–BA–Zn–BA–Zn⋯, however, the handedness of each of the two types of helices is the same in all sheets.

In this report we have witnessed considerable structural variation relating to both the stereochemistry of the metal centres and the conformations of the aldarate dianions. Despite this, there are some important structural similarities within the series. In all but one structure, two aldarate anions bind to an octahedral metal centre through a carboxylate oxygen atom and an α-hydroxyl group; the coordination environment of each metal centre is completed by either a phen or bipy ligand. In all cases parallel polymeric chains are formed with the aldarate (saccharate or mucate) bridging metal centres. Hydrogen-bonding between these chains leads to the formation of 2D sheets. The separation of the mean planes of the hydrogen bonded sheets falls within the range 12.6–13.1 Å for all compounds except for the Cu containing compounds, which is in the range of 10.2–11.0 Å. The aromatic ligands extend in directions above and below the sheet allowing face-to-face π interactions to occur between neighbouring sheets. In each structure, except for Zn(sacc)bipy, this π stacking involves aromatic groups of alternating orientation, an arrangement that leads to the formation of narrow channels bordered by the hydrogen bonded sheets at the top and bottom and the aromatic groups on the sides. This structural investigation points to three factors that appear to govern this assembly of this series of crystals. Firstly, the occupation of two coordination sites on the metal centres by the chelating aromatic ligands reduces the availability of coordination sites for the donor atoms of the bridging ligands, thus encouraging the formation of low dimensional structures *i.e.* 1D polymers. Secondly, the numerous hydrogen bonding donor and acceptor sites along the 1D chains leads to the formation of 2D hydrogen bonded sheets. Finally, face-to-face π interactions involving the aromatic ligands govern the relative orientations of adjacent sheets within the 3D structure.

Examination of properties

Powder diffraction and TGA. Powder diffraction patterns of all the compounds presented above except for Cu(bipy)(sacc) are

View Article Online

Published on 07 mai 2010. Downloaded on 24.02.2026 20:39:13.

consistent with those calculated from the single crystal data. In the case of Cu(bipy)(sacc), we suspect that loss of water has resulted in a change in the crystal structure. Thermogravimetric studies indicate, in each case, mass losses occurring in a stepwise fashion. Initial mass losses occur at ambient temperatures and continue up to temperatures between 20 and 130 °C. These initial mass losses are consistent with the loss of water from the hydrated compounds. Further mass losses, which begin in the range 145–200 °C, are consistent with decomposition of the ligands. Measured and calculated powder diffraction patterns as well as thermogravimetric traces are presented in the ESI†.

Gas sorption studies. Gas sorption studies were performed on the representative samples, Cu(muc)(phen) and Co(sacc)(phen).

Desolvation of the hydrated Cu(muc)(phen) was performed at a temperature of 100 °C under dynamic vacuum. The carbon dioxide sorption isotherm measured at 25 °C shows a maximum at approximately 1500 kPa (Fig. 6a). The observation of such maxima is a result of measurements not showing the absolute amount sorbed but rather the surface excess. The surface excess is the excess adsorbate present in the pores and on the surface of the adsorbent over and above that corresponding to the density of the gas in the bulk phase at a given temperature and pressure.[27] As a result, it is an underestimate of the total sorption particularly at higher pressures and thus the maximum in the absolute amount of carbon dioxide sorbed would be expected to occur at the maximum pressure. The desorption isotherm also shows a maximum in the surface excess, which again can be attributed to the measurement of surface excess. Significant hysteresis is also revealed in the measurement of the desorption isotherm *i.e.* some of the carbon dioxide sorbed at high pressures is retained by the solid as the pressure is lowered.

Not surprisingly, significantly more carbon dioxide is sorbed when the isotherm is measured at 0 °C; interestingly though, the carbon dioxide sorption isotherm now shows two distinct steps in the sorption curve. At relatively low pressures there is a rapid increase in the amount of gas sorbed that starts to plateau at ~500 kPa. At approximately 1700 kPa, a second step begins which continues until the maximum measured pressure of just over 3000 kPa. It is important to note that the graph indicates surface excess and like the 25 °C isotherm, it represents an underestimate of the absolute amount of carbon dioxide sorbed, particularly at high pressures. Hysteresis is again apparent upon measurement of the desorption isotherm, with the compound retaining the sorbed carbon dioxide as the pressure is lowered. Only at pressures approaching 200 kPa does the amount of carbon dioxide present in the host structure begin to drop significantly. The maximum in the desorption isotherm is once again attributed to the measurement of surface excess.

In the sorption isotherm measured at −15.2 °C, the double step sorption process is again apparent but the maximum pressure that can be attained is limited by the saturation pressure of carbon dioxide (2280 kPa at −15.2 °C). Thus, while at lower pressures more carbon dioxide is sorbed at −15.2 °C, the maximum amount of carbon dioxide that is sorbed is less than that achieved at 0 °C. Hysteresis is apparent once again in the desorption isotherm at −15.2 °C but due to the fact that the carbon dioxide loading did not occur to the same extent, less carbon dioxide is retained as the pressure is lowered compared to the 0 °C measurements.

An isosteric heat of sorption was determined by fitting a virial-type thermal adsorption equation to the −15.2, 0 and 25 °C surface excess sorption data (see Experimental section). At initial loading the ΔH_{sorp} value is −40.7 kJ mol^{-1} but this value decreased as the carbon dioxide loading increased. This relatively high value suggests a significant chemical interaction between the host structure and the carbon dioxide guest molecules. A similar value was obtained recently by Shimizu and co-workers ($\Delta H_{sorp} = -40.8$ kJ mol^{-1}) in an investigation of carbon dioxide sorption by a coordination polymer.[28] They attributed their

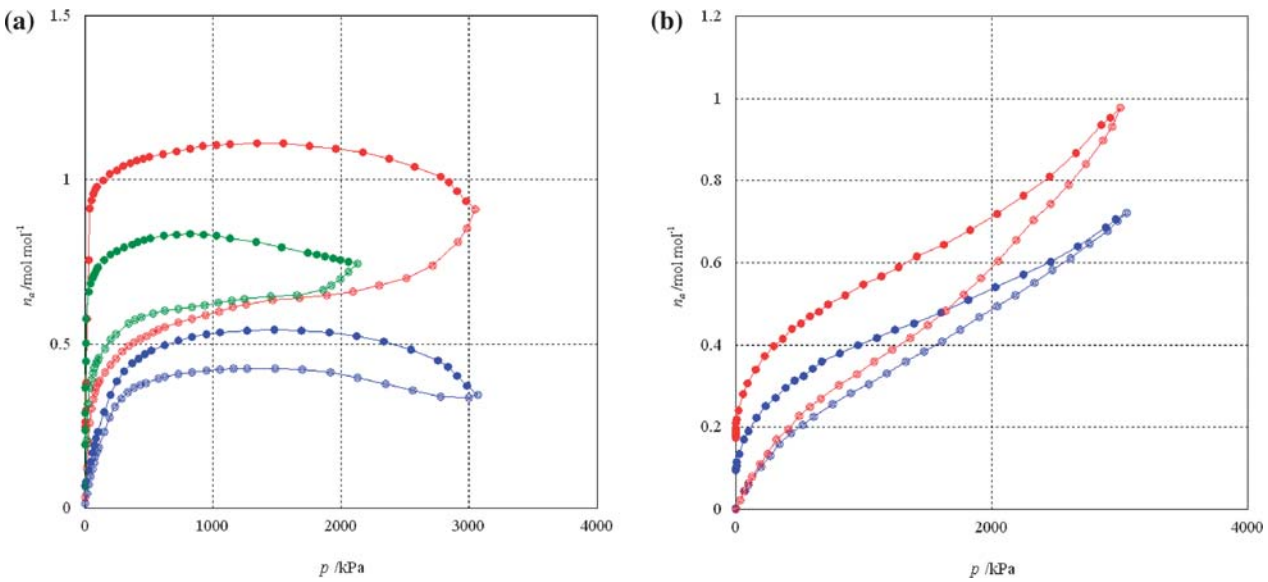

Fig. 6 Sorption and desorption isotherms for CO_2 sorption by (a) Cu(muc)(phen) −15 °C (green), 0 °C(red) and 25 °C (blue) and (b) Co(sacc)(phen) at temperatures of 0 °C (red) and 25 °C (blue). Sorption is represented by the unfilled circles, desorption by filled circles. The isotherms show the surface excess not the absolute amount of CO_2 sorbed.

 This journal is © The Royal Society of Chemistry 2010

View Article Online

Published on 07 mai 2010. Downloaded on 24.02.2026 20:39:13.

relatively high ΔH_{sorp} value to interactions between the guest molecules and non-coordinated amino groups on the network. It is possible in our compound that the hydroxyl groups of the mucate anion are interacting with carbon dioxide molecules. In support of this suggestion we note that Ferey and co-workers have proposed that carbon dioxide is capable of interacting with coordinated hydroxyl groups within a network structure. In the case of Ferey's compound $\Delta H_{sorp} = -35$ kJ mol^{-1}.[29]

While the amount of carbon dioxide sorbed by the compound is only modest (~11% by mass at 0 °C, 55 cm^3 (STP) g^{-1}), the shapes of the isotherms are interesting and perhaps suggest that a structural change occurs as the pressure increases. Such a change may result from the carbon dioxide filling the channels and forcing neighbouring sheets apart at elevated pressures. One could imagine a process in which the interdigitating π-stacked phen groups (belonging to upper and lower sheets) slide away from each other, leading to a greater separation between the hydrogen bonded sheets and an expansion of the channel cross-sectional area. We can only speculate, but a process in which the carbon dioxide molecules are re-oriented from positions where their long axes are parallel to the channel direction, to one where their long axes are vertical may be associated with the separation of the sheets. A crude estimation suggests that the sheets would need to move apart by about 0.5 Å in order to accommodate the vertical carbon dioxide molecules. The absence of the second step in the 25 °C isotherm may be an indication that a critical threshold of carbon dioxide sorption required to force the sheets apart, is not reached. In this regard we note that at high pressures there is a slight hint of a second step in the sorption isotherm at 25 °C.

Following desolvation of the hydrated Co(sacc)(phen) at a temperature of 110 °C under vacuum, the sample was able to sorb a small but significant quantity of carbon dioxide. At a temperature of 0 °C, almost 50 cm^3 of CO_2 (at STP) is sorbed per gram of compound at a pressure of 3000 kPa. This corresponds to approximately 1.0 carbon dioxide molecule sorbed per metal centre (Fig. 6b). The sorption isotherms recorded at 0 and 25 °C all show a similar shape to each other. An initial sharp rise is apparent but instead of the isotherms levelling out, the amount of carbon dioxide sorbed continues to rise. In the case of the −15 and 0 °C isotherms the gradient of the isotherm even starts to increase at higher pressures. As with Cu(muc)(phen) we can only speculate on the reasons for this behaviour but it seems likely to be linked to some degree of fexibility within the crystal. Perhaps as the channels become filled with carbon dioxide, the channel walls are forced further apart allowing the sorption of further carbon dioxide. Unlike Cu(muc)(phen), the 1-D polymer in Co(sacc)(phen) is far from linear and therefore the expansion of the channels may be linked to the zig-zag chains becoming closer to linear. We note that Kitagawa *et al.* have proposed that an adsorption isotherm may have a novel profile, dissimilar to the conventional types, if the host has a flexible and dynamic nature.[30]

The reason for the hysteresis apparent in the isotherms for both compounds is uncertain but it may be due to the relatively narrow, non-intersecting channels allowing only sluggish diffusion of the guest molecules. A similar explanation for hysteresis has been offered by Seo and Chun in their investigation of a coordination polymer possessing narrow channels.[31]

Sorption measurements involving nitrogen, hydrogen (both at 77 K) and methane (at −15.2 °C) on both compounds indicated that negligible quantities of these gases were sorbed.

Experimental section

Mucic acid (galactaric acid) and the enantiomerically pure, potassium hydrogen D-saccharate (potassium hydrogen D-glucarate) were obtained from commercial sources and were used without further purification. The coordination polymers were obtained from hot aqueous solutions of the appropriate metal salts and ligands as indicated below.

Mn(sacc)(phen)·2H$_2$O

Potassium hydrogen saccharate (20 mg, 0.081 mmol) and 1,10-phenanthroline hydrate (15 mg, 0.083 mmol) were dissolved in hot water (4 mL). This solution was added to $Mn(OAc)_2 \cdot 4H_2O$ (20 mg, 0.082 mmol) in water (1 mL) and held at 73 °C overnight. Yellow plate crystals formed directly from the hot solution (21 mg, 53% yield). IR (KBr) 3400 (br), 2937, 2349, 1656, 1599, 1517, 1493, 1424, 1385, 1358, 1296, 1266, 1221, 1137, 1111, 1100, 1084, 1055, 1024, 981, 940, 865, 850, 780, 727, 700, 635 cm^{-1}. Anal. Calcd for $Mn(C_6H_8O_8)(C_{10}H_8N_2) \cdot 2H_2O$: C 45.11, H 4.21, N 5.84%. Found: C 45.12, H 4.16 N, 5.86%.

Zn(sacc)(phen)·2H$_2$O

The best crystals were obtained by mixing solutions of potassium hydrogen saccharate (20 mg, 0.081 mmol) and 1,10-phenanthroline hydrate (15 mg, 0.083 mmol) in hot water (6 mL) and $Zn(NO_3)_2 \cdot 6H_2O$ (145 mg, 0.49 mmol) in water (1 mL). Colourless plate crystals formed directly from the hot solution in extremely low yield (<1 mg). Larger yields were obtained by heating a solution of potassium hydrogen saccharate (20 mg, 0.081 mmol), 1,10-phenanthroline hydrate (20 mg, 0.081 mmol) and $Zn(NO_3)_2 \cdot 6H_2O$ (29 mg, 0.097 mmol) in hot water (9 mL). Crystals exhibiting severe twinning (16 mg, 40% yield) were obtained directly from the hot solution, collected and washed with water. IR (KBr) 3396 (br), 1654, 1599, 1518, 1425, 1384, 1265, 1223, 1138, 1102, 1059, 1027, 942, 869, 851, 782, 725, 638, 576, 522, 495, 481, 423 cm^{-1}. Anal. Calcd for $Zn(C_6H_8O_8)(C_{10}H_8N_2) \cdot 2H_2O$: C 44.14, H 4.12, N 5.72%. Found: C 44.22, H 4.09, N 5.67%.

Co(sacc)(phen)·2H$_2$O

Potassium hydrogen saccharate (20 mg, 0.081 mmol) and 1,10-phenanthroline hydrate (15 mg, 0.083 mmol) were dissolved in hot water (2 mL). $Co(OAc)_2 \cdot 4H_2O$ (20 mg, 0.082 mmol) in water (1 mL) was added to this solution and the mixture held at 73 °C overnight. Pink plate crystals formed directly from the hot solution (23 mg, 59% yield). IR (KBr) 3405 (br), 1654, 1596, 1517, 1424, 1384, 1266, 1136, 1112, 1102, 1084, 1057, 869, 850, 780, 725, 639, 576, 520, 481 cm^{-1}. Anal. Calcd for $Co(C_6H_8O_8)(C_{10}H_8N_2) \cdot 2H_2O$: C 44.73, H 4.17, N 5.80%. Found: C 44.91, H 4.18, N 5.84%.

View Article Online

Published on 07 mai 2010. Downloaded on 24.02.2026 20:39:13.

Cd(muc)(phen)·2H_2O

1,10-Phenanthroline hydrate (15 mg, 0.083 mmol) suspended in an aqueous solution (6 mL) of mucic acid (17 mg, 0.081 mmol), cadmium acetate dihydrate (20 mg, 0.075 mmol) and potassium hydroxide (160 μL (1 M), 0.16 mmol) was left to stand overnight at 87 °C. Colourless leaf-shaped crystals (23 mg, 57% yield) formed directly from the hot solution. IR (KBr) 3440 (br), 3178 (br), 2936, 1652, 1591, 1518, 1493, 1454, 1430, 1384, 1317, 1267, 1221, 1139, 1108, 1099, 1034, 980, 876, 865, 849, 841, 779, 725, 663, 642, 546, 479, 420 cm^{-1}. Anal. Calcd for $Cd(C_6H_8O_8)(C_{10}H_8N_2)\cdot 2H_2O$: C 40.28, H 3.76, N 5.22%. Found: C 40.38, H 3.70, N 5.24%.

Cu(muc)(phen)·3H_2O

1,10-Phenanthroline hydrate (15 mg, 0.083 mmol) was suspended in an aqueous solution (6 mL) of dipotassium mucate (24 mg, 0.078 mmol) and copper nitrate trihydrate (20 mg, 0.083 mmol). The mixture was held at 87 °C overnight and afforded blue, wedge-shaped crystals (18 mg, 44% yield) directly from the hot solution. IR (KBr) 3374 (br), 2891, 2361, 1609, 1571, 1522, 1429, 1382, 1344, 1300, 1248, 1201, 1150, 1111, 1040, 975, 875, 855, 842, 725, 674, 649, 567, 496 cm^{-1}. Anal. Calcd for $Cu(C_6H_8O_8)(C_{10}H_8N_2)\cdot 3H_2O$: C 42.73, H 4.38, N 5.54%. Found: C 42.86, H 4.39, N 5.56%.

Cu(sacc)(bipy)·1.5H_2O

Copper acetate monohydrate (199 mg, 0.996 mmol), potassium hydrogen saccharate (250 mg, 1.01 mmol) and 2,2′-bipyridine (155 mg, 0.992 mmol) were dissolved in hot water (16 mL). The mixture was left to stand overnight at 80 °C. Blue needle crystals (294 mg, 29% yield) separated from the cooled reaction mixture over several days. IR (KBr) 3566, 3462, 3408, 3201, 3110, 3078, 3062, 3036, 2946, 1660, 1622, 1600, 1495, 1476, 1447, 1430, 1404, 1367, 1319, 1287, 1253, 1240, 1224, 1195, 1176, 1160, 1126, 1103, 1088, 1058, 1033, 990, 952, 897, 873, 836, 780, 759, 732, 686, 661, 588, 546, 489, 417 cm^{-1}. Anal. Calcd for $Cu(C_6H_8O_8)(C_8H_8N_2)\cdot 1.5H_2O$: C 42.25, H 4.21, N 6.16%. Found: C 42.04, H 4.18, N 6.05%.

Zn(sacc)(bipy)·3H_2O

An aqueous solution (20 mL) of potassium hydrogen saccharate (80 mg, 0.32 mmol), 2,2′-bipyridine (52 mg, 0.39 mmol) and $Zn(OAc)_2\cdot 2H_2O$ (72 mg, 0.328 mmol) was left to stand at 87 °C overnight. Colourless block crystals (<1 mg) formed from standing of the reaction mixture over several weeks. For higher yields, KHsacc (20 mg, 0.081 mmol), 2,2′-bipyridine (13 mg, 0.083 mmol) and $Zn(OAc)_2\cdot 2H_2O$ (20 mg, 0.091 mmol) were dissolved in 2 mL distilled water and heated to 84 °C overnight to give a larger mass of twinned crystals (3 mg, 4% yield) directly from the hot solution. IR (KBr) 3412 (br), 1607, 1598, 1494, 1477, 1444, 1374, 1323, 1253, 1180, 1156, 1120, 1091, 1063, 1027, 956, 881, 843, 768, 736, 653, 632, 484, 414 cm^{-1}. Anal. Calcd for $Zn(C_6H_8O_8)(C_8H_8N_2)\cdot 3H_2O$: C 39.73, H 4.58, N 5.79%. Found: C 39.82, H 4.41, N 5.76%.

Infrared spectra were recorded using a BioRad 175 FTIR spectrometer. Elemental analyses were performed by the Campbell Microanalytical Laboratory, University of Otago, New Zealand.

Crystallography

Crystal data and refinement details are presented in Table 1. In each case crystals were transferred directly from the mother liquor to a protective oil prior to cooling on the diffractometer. Data for all the compounds except Cu(sacc)(bipy) were measured on a Oxford Diffractometer Excalibur diffractometer fitted with CuKα radiation while data for Cu(sacc)(bipy) were measured on a Bruker SMART CCD diffractometer fitted with MoKα radiation. The structures were solved using direct methods and refined using a full-matrix least-squares procedure based on F^2. Solution and refinement were performed using SHELX-97[32] within the WinGX suite of programs.[33]

Gas sorption measurements

Gas sorption data were measured using a Sieverts-type BELsorp-HP automatic high pressure gas sorption apparatus (BEL Japan Inc.). Ultra-high purity CH_4, CO_2, H_2, He and N_2 used for sorption studies were purchased from BOC or Air Liquide. Non-ideal gas behaviour at high pressures was corrected for by fitting second-order virial equations to curves of compression factor Z *vs.* pressure (0 to 3.5 MPa) for each gas at each measurement and reference temperature, plotted from data obtained from the NIST fluid properties website.[34] Sample temperatures were controlled by a Julabo F25-ME chiller/heater that recirculated fluid at ±0.1 °C through a capped, jacketed stainless steel flask containing ethanol, kept within a polystyrene foam box. A calibrated external Pt100 temperature probe monitored the ethanol temperature. Samples were kept at the measurement temperature for a minimum of 1 h after the desired temperature had been achieved to allow full thermal equilibrium to be attained before data measurement commenced. Isosteric heats of sorption were calculated using a virial-type thermal adsorption equation that modelled ln P as a function of amount of surface excess of gas sorbed over the measurement temperatures.[35] Only data up to and including the maximum surface excess were modelled. Equilibrium pressure values were measured such that the stability criterion of 15 continuous minutes with a pressure change of less than the greater of 0.35 kPa or 0.1%. Lower equilibrium time measurements showed considerably more hysteresis. Analyses were performed using the BELMaster (BEL Japan Inc.) software package.

Acknowledgements

We gratefully acknowledge the financial support of the Australian Research Council.

References

1 T. Taga, Y. Kuroda and K. Osaki, *Bull. Chem. Soc. Jpn.*, 1977, **50**, 3079.
2 T. Taga and K. Osaki, *Bull. Chem. Soc. Jpn.*, 1976, **49**, 1517.
3 F. Ferrier, A. Avezou, G. Terzian and D. Benlian, *J. Mol. Struct.*, 1998, **442**, 281.
4 T. Taga, T. Shimada and N. Mimura, *Acta Crystallogr., Sect. C: Cryst. Struct. Commun.*, 1994, **50**, 1076.

 This journal is © The Royal Society of Chemistry 2010

View Article Online

5 C. Burden, W. Mackie and B. Sheldrick, *Acta Crystallogr., Sect. C: Cryst. Struct. Commun.*, 1985, **41**, 693.
6 B. Sheldrick and W. Mackie, *Acta Crystallogr., Sect. C: Cryst. Struct. Commun.*, 1989, **45**, 1072.
7 B. Sheldrick, W. Mackie and D. Akrig, *Acta Crystallogr., Sect. C: Cryst. Struct. Commun.*, 1989, **45**, 191.
8 W. Tian, S. Cheng, L.-M. Yang, X.-L. Jin, S.-F. Weng and J.-G. Wu, *J. Inorg. Biochem.*, 2000, **78**, 197.
9 W. Tian, H. Liao, J.-G. Wu and G.-D. Yang, *Polyhedron*, 1997, **16**, 2055.
10 G. Wang, Y. Fan, L. Hong, H. Guo, J. Wu and G. Xu, *Acta Sci. Nat. Univ. Pekin.*, 1988, **24**, 385.
11 K.-L. Wong, G.-L. Law, Y.-Y. Yang and W.-T. Wong, *Adv. Mater.*, 2006, **18**, 1051.
12 S. D. Styron, A. D. French, J. D. Friedrich, C. H. Lake and D. E. Kiely, *J. Carbohydr. Chem.*, 2002, **21**, 27.
13 A. Lakatos, R. Bertani, T. Kiss, A. Venzo, M. Casarin, F. Benetollo, P. Ganis and D. Favretto, *Chem.–Eur. J.*, 2004, **10**, 1281.
14 M. Kato, A. K. Sah, T. Tanase and M. Mikuriya, *Inorg. Chem.*, 2006, **45**, 6646.
15 P. Klufers, G. Kramer, H. Piotrowski and J. Senker, *Z. Naturforsch., B: Chem. Sci.*, 2002, **57**, 1446.
16 F. Benetollo, G. Bombieri, H. Liang, H. Liao, N. Shi and J. Wu, *J. Crystallogr. Spectrosc. Res.*, 1993, **23**, 171.
17 G. A. Jeffrey and R. A. Wood, *Carbohydr. Res.*, 1982, **108**, 205.
18 E. Ferrari and M. Saladini, *J. Inorg. Biochem.*, 2004, **98**, 1002.
19 M. L. Ramos, M. M. Caldiera, V. M. S. Gil, H. van Bekkum and J. A. Peters, *J. Coord. Chem.*, 1994, **33**, 319.
20 M. L. Ramos, M. M. Caldiera, V. M. S. Gil, H. van Bekkum and J. A. Peters, *Polyhedron*, 1994, **13**, 1825.
21 M. Saladini, L. Menabue and E. Ferrari, *Carbohydr. Res.*, 2001, **336**, 55.
22 M. Saladini, E. Ferrari and L. Menabue, *J. Inorg. Biochem.*, 2002, **92**, 121.
23 B. F. Abrahams, M. Moylan, S. D. Orchard and R. Robson, *Angew. Chem., Int. Ed.*, 2003, **42**, 1848.
24 B. F. Abrahams, M. Moylan, S. D. Orchard and R. Robson, *CrystEngComm*, 2003, **5**, 313.
25 M. Saladini, M. Candini, D. Iacopino and L. Menabue, *Inorg. Chim. Acta*, 1999, **292**, 189.
26 A. C. Fabretti, G. Franchini, P. Zannini and M. Di Vaira, *Inorg. Chim. Acta*, 1985, **105**, 187.
27 P. G. Menon, *Chem. Rev.*, 1968, **68**, 277.
28 R. Vaidhyanathan, S. S. Iremonger, K. W. Dawson and G. K. H. Shimizu, *Chem. Commun.*, 2009, 5230.
29 S. Bourrelly, P. L. Llewellyn, C. Serre, F. Millange, T. Loiseau and G. Ferey, *J. Am. Chem. Soc.*, 2005, **127**, 13519.
30 S. Shimomoura, S. Bureekaew and S. Kitagawa, in *Molecular Networks, Structure and Bonding*, Vol. ed. M. W. Hosseini, Ser. ed. D. M. P. Mingos, Springer-Verlag, Berlin, Heidelberg, 2009, vol. 132, p. 51.
31 J. Seo and H. Chun, *Eur. J. Inorg. Chem.*, 2009, 4946.
32 G. M. Sheldrick, *SHELX-97, Program for Crystal Structure Analysis*, University of Gottingen, Germany, 1997.
33 L. J. Farrugia, *J. Appl. Crystallogr.*, 1999, **32**, 837.
34 http://webbook.nist.gov/chemistry/fluid/.
35 L. Czepirski and J. Jagiello, *Chem. Eng. Sci.*, 1989, **44**, 797.

Published on 07 mai 2010. Downloaded on 24.02.2026 20:39:13.